

ChemComm

Accepted Manuscript



This is an *Accepted Manuscript*, which has been through the Royal Society of Chemistry peer review process and has been accepted for publication.

Accepted Manuscripts are published online shortly after acceptance, before technical editing, formatting and proof reading. Using this free service, authors can make their results available to the community, in citable form, before we publish the edited article. We will replace this *Accepted Manuscript* with the edited and formatted *Advance Article* as soon as it is available.

You can find more information about *Accepted Manuscripts* in the [Information for Authors](#).

Please note that technical editing may introduce minor changes to the text and/or graphics, which may alter content. The journal's standard [Terms & Conditions](#) and the [Ethical guidelines](#) still apply. In no event shall the Royal Society of Chemistry be held responsible for any errors or omissions in this *Accepted Manuscript* or any consequences arising from the use of any information it contains.

COMMUNICATION

Protein-Based Fluorescent Metal Nanoclusters for Small Molecular Drug Screening

Cite this: DOI: 10.1039/x0xx00000x

Yong Yu,^{a, ‡} Siu Yee New,^{a, ‡, §} Jianping Xie,^b Xiaodi Su,^{*, a} and Yen Nee Tan^{*, a}

Received 00th January 2012,

Accepted 00th January 2012

DOI: 10.1039/x0xx00000x

www.rsc.org/

A facile drug screening method based on synthesizing fluorescent gold nanoclusters inside albumin proteins loaded with small molecular drugs and comparing the relative fluorescence intensities of the resultant gold nanoclusters has been developed and successfully applied for the quantitative measurement of drug-protein binding constant.

Noble metal nanoclusters (NCs) are generally defined as ultrasmall (< 2 nm) particles consisting of several to a few hundreds of metal (Au, Ag) atoms.¹⁻³ Due to the strong quantum confinement in the sub-2 nm size regime, metal NCs possess discrete and size-dependent electronic structure and exhibit unique molecular-like properties, such as quantized charging,⁴⁻⁵ magnetism,⁶ and strong fluorescence,⁷⁻¹¹ which are not observed in single atoms nor crystalline metal nanoparticles (> 2 nm)¹²⁻¹⁵. To date, several different synthetic strategies have been developed for the formation of fluorescent metal NCs.¹⁶⁻²⁶ In particular, biomolecules (e.g., protein¹⁶ and peptide¹⁷⁻¹⁸) templated Au NCs have attracted increasing research interests owing to their excellent photostability, ultrasmall size, low toxicity, and good biocompatibility. These advantageous properties have rendered this new type of fluorophore ideal optical probes for biosensing and imaging applications.²⁷⁻³²

The formation of protein-based Au NCs usually relies on the biomineralizing properties of the functional proteins themselves. In a typical protein-directed synthesis, gold precursors (Au ions) are firstly encapsulated within the protein molecule, followed by a slow reduction process enabled by certain amino acid residues, such as tyrosine,^{16, 33} and tryptophan,³⁴ that can function as mild reducing agents at appropriate conditions (e.g., alkaline pH) to allow the formation of Au NCs within the protein template. For a given protein template, the accessibility of tyrosine residues for the formation of Au NCs is determined by the degree of protein unfolding. It can thus be rationalized that the kinetics of fluorescent metal NC formation could be controlled by manipulating the unfolding process of the protein. One way to control protein

unfolding is to use reaction conditions that lead to protein denaturing (e.g., heat-treatment or exposure to denaturing agents). Previous studies have demonstrated that the formation process of the fluorescent Au NCs directed by bovine serum albumin (BSA) can be shortened from 48 h to 12 h by raising the reaction temperature from 25 °C to 37 °C.¹⁶ This is due to the denaturation/unfolding event of the protein at the higher temperature that causes more functional tyrosine residues to be exposed for the encapsulated gold ions and thereafter leading to a higher reduction/reaction rate. Similarly, the presence of denaturing agents can also promote the protein unfolding process and thus accelerate the reaction rate of the formation of metal NCs. While a given protein has a defined thermal stability, binding of small molecules to the protein usually induces changes in protein thermal stability with modification of the midpoint denaturation temperature and enthalpy of unfolding.³⁵⁻³⁶ Furthermore, different ligands may have different binding affinity to the protein at defined binding sites. The strategy, as for how the ligand binds to a specific protein may affect the kinetics of protein-templated Au NC formation, has not been investigated before.

Herein we report the preparation of Au NCs using ligand-bound protein under heat treatment and further render this strategy as a new and ubiquitous method for small molecular drug screening. The success of this method for drug screening is built upon the fact that drugs or ligands of different binding affinities to the protein template can lead to different stabilization effect against the heat-induced protein unfolding. Those drugs with stronger binding affinities will stabilize the protein better, leading to lesser protein unfolding, and thus a slower formation rate of Au NCs. With a naturally-occurring globular protein, human serum albumin (HSA), and four small molecular drugs (e.g., ibuprofen, warfarin, phenytoin, and sulfanilamide) as examples, we have demonstrated the detection of ligand binding to HSA and the screening of relative affinity of the four ligands to this protein by simply comparing the difference in fluorescence intensity among Au NCs synthesized at 60 °C³⁷ within protein templates loaded with the ligands. The fluorescence intensity has an inverse relationship with the binding affinities of different

drugs interacting with the target protein, e.g., HSA loaded with high affinity ligands will result in fewer amount of Au NCs formed within the template and thus lower fluorescence intensity is observed; and *vice versa*. Furthermore, through titration of protein ligand at different concentrations, we can determine the binding constant of drugs in homogenous solution during the *in-situ* synthesis of Au NCs without the use of sophisticated instruments. To prove the generality and the quantitative nature of this method, we have further proven the concept using another serum albumin protein (BSA) and warfarin as drug ligand. To the best of our knowledge, this is the first attempt to couple protein's biofunctionality (i.e. drug binding activity) with the protein-templated Au NC synthesis for biosensing. The synergistic application of the dual properties of a protein introduces new material strategy for controlled NC synthesis and hitherto unreported analytical science concept for rapid drug screening.

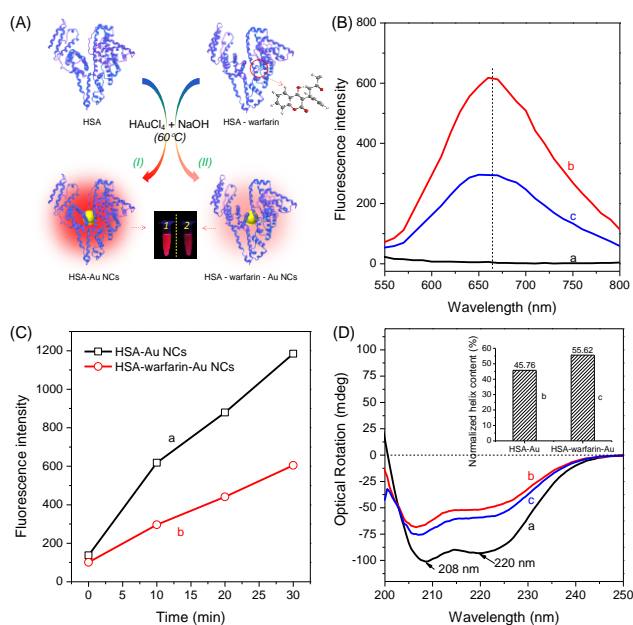


Figure 1. (A) Schematic of Au NCs formed by using (I) HSA and (II) HSA-warfarin as templates. (B) Photoemission spectra of HSA-Au NCs prepared at (a) room temperature, (b) 60 °C, and (c) HSA-warfarin-Au NCs prepared at 60 °C (all were measured at 10 minutes upon addition of NaOH). (C) Time resolved fluorescence intensity at 670 nm of (a) HSA-Au NCs and (b) HSA-warfarin-Au NCs. (D) Far-UV CD spectra of (a) HSA, (b) HSA-Au NCs, and (c) HSA-warfarin-Au NCs. (Inset) The calculated α -helix content of HSA-Au and HSA-warfarin-Au NCs.

HSA is predominantly a helical protein with 585 amino acid residues, 18 of which are tyrosine residues that can be utilized to reduce the encapsulated Au ions. Meanwhile, HSA is composed of three similar domains (I-III) and two main drug binding sites, i.e., subdomain IIA (Sudlow's site I) and IIIA (Sudlow's site II) that can bind to a wide range of poorly soluble drugs.³⁸ Figure 1A shows the schematic illustration on how the drug screening can be carried out through the *in-situ* synthesis of fluorescent Au NCs directed by the HSA template under heat treatment. Typically, the HSA-Au NCs were synthesized by adding aqueous solutions of HSA and gold precursors (HAuCl₄) to the preheated ultrapure water at 60 °C for 10 min, followed by an addition of NaOH to bring the solution pH to alkaline (10.5) in order to trigger the reduction capability of tyrosine

residues of the protein for the formation of Au NCs within the template (Figure 1A, route I). The as-synthesized HSA-Au NCs show a bright red fluorescence under the UV light (Figure 1A, item I), exhibiting a distinct peak at 670 nm of the emission spectrum (Figure 1B, red line). On the other hand, HSA was pre-loaded with drug molecules prior to use as the template for the synthesis of Au NCs under the same reaction conditions (see Figure 1A, route II for the warfarin-bound HSA as an example). It can be seen that a lower intensity of HSA-warfarin-Au NCs (Figure 1B, blue line) was formed under the reaction time (i.e., 10 min) as that of HSA-Au NCs (Figure 1B, red line). The time course fluorescence intensity in Figure 1C clearly shows that the formation process of HSA-warfarin-Au NCs is slower than that of the HSA-Au NCs, suggesting that the ligand-bound protein is more stable against unfolding from heat-treatment. Therefore, by comparing the fluorescence intensity of Au NCs formed at a fixed reaction time, the protein-drug binding interaction could be identified.

Through a comprehensive study of Au NCs formed, both with and without drug loading involving UV-vis spectroscopy, photoluminescence spectroscopy, matrix-assisted laser desorption ionization - time of flight (MALDI-TOF) mass spectrometry and circular dichroism (CD), we have confirmed that the binding of drug to the serum albumin only affects the formation kinetics but not the size/structure of the resultant Au NCs. Particularly, the optical absorption spectra of HSA-Au NCs and HSA-warfarin-Au NCs show only several small bumps in the visible range (Figure S2). No surface plasmon resonance (SPR) peaks have been observed, which rules out the possibility of forming large Au nanoparticles and confirms the formation of Au NCs. The photoexcitation spectra of the HSA-Au NCs and HSA-warfarin-Au NCs all show a major peak at 370 nm and two less prominent peaks at 480 and 500 nm (Figure S3). Together with the photoemission spectra (Figure 1B), the same photoluminescence properties of the HSA-Au NCs and HSA-warfarin-Au NCs suggest that their cluster sizes/structures are similar. MALDI-TOF mass spectrometry was also carried out to determine the size of the HSA-Au NCs and HSA-warfarin-Au NCs (Figure S4). The spectrum of HSA-warfarin-Au NCs is superimposable to that of the HSA-Au NCs, which also confirms the size of HSA-warfarin-Au NCs is similar to that of the HSA-Au NCs. The molecular weight of warfarin (MW308.33) is relatively small and might not be resolved in MALDI-TOF measurements. In addition, CD was employed to investigate the stabilizing effect of drug to HSA protein structure in affecting the formation kinetics of Au NCs inside HSA-drug templates. The far-CD spectra in Figure 1d shows that 54.24% of α -helical structure was lost during the formation of HSA-Au NCs at 60 °C, which is the result of protein denaturation caused by heat treatment. By replacing the HSA with the warfarin loaded-HSA, 55.62% of α -helical structure of HSA is retained (i.e. 44.38% lost). The lesser α -helical loss (by 9.86%) confirms the stabilizing ability of the drug to HSA that retards the unfolding process. With this experiment, we have shown that the formation kinetics of Au NCs is highly sensitive to the protein structure, and even such subtle difference in α -helical content (9.86%) is profound enough to result in different formation rate of Au NCs. This observation has laid the basis to use the Au NCs formation kinetics (or the intensity at a fixed reaction time) to screen drugs of different affinities (*vide infra*).

To demonstrate the ability of this method for small molecular drug screening based on fluorescence intensities of the resultant HSA-drug-Au NCs, a total of four ligands with different binding affinities and drug binding sites on the HSA were tested (Table S1). Ibuprofen is known to bind to drug binding site II, whereas the rest

bind to site I with different affinities. The time resolved photoemission spectra of the different HSA-drug-Au NCs were shown in Figure S1. As can be seen in Figure 2A, the sample without ligand (control) shows the highest intensity amongst all, followed by those with sulfanilamide, phenytoin, warfarin, and ibuprofen sequentially. This fluorescence intensity trend is inversely proportional to the binding strength of three of the four drugs of which the binding constants (K_D) have been determined in a previous homogenous-phased NMR study (Table S1), i. e., phenytoin ($131.6 \pm 12.5 \mu\text{M}$), warfarin ($4.0 \pm 2.8 \mu\text{M}$), ibuprofen ($0.5 \pm 1.0 \mu\text{M}$).³⁹ The inverse relationship between fluorescence intensity and binding affinity confirms our hypothesis that drugs with stronger binding affinities (smaller K_D) can stabilize the protein better against denaturation during the formation of fluorescent Au NCs at 60 °C. Sulfanilamide is known to bind to Sudlow's site I, but its K_D has yet to be reported. Our results suggest that sulfanilamide has the weakest binding affinity to HSA among all drugs tested in this study. In addition, the intensity trend shown in Figure 2A is reproducible for multiple experiments (Figure 2B), which confirms the reliability of our fluorescence assay to screen for the relative HSA-drug binding affinity in a rapid manner simply based on the fluorescence intensity difference of resultant HSA-drug-Au NCs. Also, the brightness of these Au NCs can be easily differentiated by naked-eyes (Figure 2B, inset), which highlights the feasibility of using current methodology for a convenient, fast, equipment-free screening of different drugs.

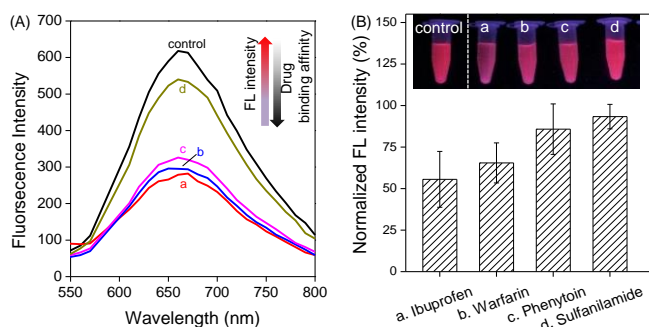


Figure 2. (A) Photoemission spectra of HSA-Au NCs prepared at 60 °C in the presence of different drugs. Control experiment was carried out in the absence of any drugs. (B) Normalized photoemission intensity of HSA-drug-Au NCs against HSA-Au NCs (control). Both spectra and digital photos (inset of B) were taken at 10 min after addition of NaOH at 60 °C.

Driven by the consistent trend obtained on the relative binding affinity of drug ligands to HSA, we further modified the Au NC-drug screening protocol for the quantitative measurement of K_D . As a demonstrative example, we have selected warfarin and ibuprofen (which are known as a site I and a site II drug, respectively) as model ligands to measure K_D . By varying the amount of ligand used for pre-incubation with HSA, the fluorescence intensity of the resultant Au NCs synthesized at 60 °C was recorded and used to calculate the K_D value by fitting with the Michaelis-Menten equation: $Y = R_{\text{max}} \times C / (K_D + C)$, where R_{max} indicates the maximum response signal, C is the concentration of ligand and K_D is the binding constant. As shown in Figure 3A and 3B, fluorescence intensity of the as-synthesized HSA-drug-Au NCs decreases as the amount of ligand increases, which corroborates the enhancement of HSA stability against unfolding (induced by thermal treatment) in the presence of increased amount of ligand. In other words, the increased amount of ligand provides a higher stability of HSA

against thermal denaturation that results in the formation of limited amount of Au NCs detected at lower fluorescence intensity. The K_D of warfarin and ibuprofen were calculated to be $10.12 \pm 2.06 \mu\text{M}$ and $0.74 \pm 0.1 \mu\text{M}$, respectively. These values are comparable to those measured from NMR study³⁹ ($4.0 \pm 2.8 \mu\text{M}$ and $0.5 \pm 1.0 \mu\text{M}$) (Figure 3C), which confirms the reliability of the current method to quantify binding constants of different HSA-binding drugs in homogenous solution.

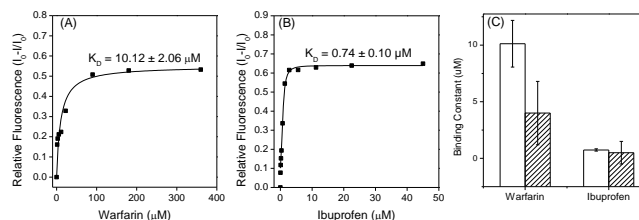


Figure 3. K_D measurement using dose response plots. (A) HSA-warfarin-Au NCs and (B) HSA-ibuprofen-Au NCs synthesized by pre-incubated HSA-drug template at 60 °C with increasing amount of drugs. The data was fitted to a single site binding model using OriginPro 8. (C) K_D values determined in this study (open bar) as compared with those previously reported values (slash patterned bar).

To demonstrate the generality and the quantitative nature of our drug screening assay, we have performed the drug binding test for bovine serum albumin (BSA), another type of albumin protein which shares the highly similar homology (88%) with HSA, and measured the binding constant of warfarin to BSA. Using the same experimental protocol, BSA was able to form fluorescent Au NCs in the absence and presence of warfarin, exhibiting an intense red emission at 680 nm (Figure S5). Using the similar titration method, we have calculated K_D of warfarin with BSA ($3.41 \pm 2.03 \mu\text{M}$). This value was quite close to the K_D of warfarin with HSA reported in literature ($4.0 \pm 2.8 \mu\text{M}$)³⁹ from NMR studies, which was not unexpected considering the highly similar homology of these two albumin proteins.

In conclusion, we have developed a simple, fast (~10 min), and straightforward method to detect the binding of small molecular drugs to protein and to screen the relative affinity of various protein binding drugs by monitoring the formation kinetics of fluorescent Au NCs inside the protein-drug templates. Our design took the advantage of the stabilizing effect of various serum albumin-binding drugs against protein unfolding event that affects the formation kinetics of fluorescent Au NCs. The stronger a drug binds to the protein, the slower formation rate of the fluorescent Au NCs would have, leading to an inverse correlation between the fluorescence intensity and binding affinity of drug. Drug screening was therefore carried out by the simple observation of fluorescence intensity difference of the as-synthesized Au NCs. In addition to detecting drug binding and screening relative affinity, our method can further quantify the drug-protein binding affinity constant. Several drugs with a wide range of binding affinities (e.g., ibuprofen, warfarin, phenytoin, and sulfanilamide) to HSA and BSA have been used to demonstrate the concepts and to confirm the generality and quantitative nature of our method.

Acknowledgement

Y.N.T. would like to acknowledge the Agency for Science, Technology and Research (A*STAR), Singapore for the financial support under the JCO CDA grant 13302FG063.

Notes and references

^a Institute of Materials Research and Engineering, 3 Research Link, Singapore 117602. Email: tanyn@imre.a-star.edu.sg (Y.N.T.), xd-su@imre.a-star.edu.sg (X.S.); Tel: +65 6874 7091

^b Department of Chemical and Biomolecular Engineering, National University of Singapore, 10 Kent Ridge Crescent, Singapore 119260

‡ These authors contributed equally to this work.

§ Present Address: School of Pharmacy, Faculty of Science, University of Nottingham, Malaysia Campus, Jalan Broga, 43500 Semenyih, Selangor Darul Ehsan, Malaysia.

† Electronic Supplementary Information (ESI) available: Experimental details and supporting figures. See DOI: 10.1039/c000000x/

- 1 Lu, Y.; Chen, W. *Chem. Soc. Rev.* **2012**, 41, 3594.
- 2 Kim, B. H.; Hackett, M. J.; Park, J.; Hyeon, T. *Chem. Mater.* **2013**, 26, 59.
- 3 Yu, Y.; Yao, Q.; Luo, Z.; Yuan, X.; Lee, J. Y.; Xie, J. *Nanoscale* **2013**, 5, 4606.
- 4 Murray, R. W. *Chem. Rev.* **2008**, 108, 2688.
- 5 Laaksonen, T.; Ruiz, V.; Liljeroth, P.; Quinn, B. M. *Chem. Soc. Rev.* **2008**, 37, 1836.
- 6 Zhu, M.; Aikens, C. M.; Hendrich, M. P.; Gupta, R.; Qian, H.; Schatz, G. C.; Jin, R. *J. Am. Chem. Soc.* **2009**, 131, 2490.
- 7 Lin, C.-A. J.; Yang, T.-Y.; Lee, C.-H.; Huang, S. H.; Sperling, R. A.; Zanella, M.; Li, J. K.; Shen, J.-L.; Wang, H.-H.; Yeh, H.-I.; Parak, W. J.; Chang, W. H. *ACS Nano* **2009**, 3, 395.
- 8 Udaya Bhaskara Rao, T.; Pradeep, T. *Angew. Chem., Int. Ed.* **2010**, 49, 3925.
- 9 Luo, Z.; Yuan, X.; Yu, Y.; Zhang, Q.; Leong, D. T.; Lee, J. Y.; Xie, J. *J. Am. Chem. Soc.* **2012**, 134, 16662.
- 10 Guével, X.; Spiess, C.; Daum, N.; Jung, G.; Schneider, M. *Nano Res.* **2012**, 5, 379.
- 11 Yu, Y.; Luo, Z.; Chevrier, D. M.; Leong, D. T.; Zhang, P.; Jiang, D.-e.; Xie, J. *J. Am. Chem. Soc.* **2014**, 136, 1246.
- 12 Yang, J.; Lee, J. Y.; Ying, J. Y. *Chem. Soc. Rev.* **2011**, 40, 1672.
- 13 Lu, C.-H.; Wang, Y.-W.; Ye, S.-L.; Chen, G.-N.; Yang, H.-H. *NPG Asia Mater.* **2012**, 4, e10.
- 14 Li, Y.; Zaluzhna, O.; Xu, B.; Gao, Y.; Modest, J. M.; Tong, Y. J. *J. Am. Chem. Soc.* **2011**, 133, 2092.
- 15 Wei, H.; Wang, Z.; Zhang, J.; House, S.; Gao, Y.-G.; Yang, L.; Robinson, H.; Tan, L. H.; Xing, H.; Hou, C.; Robertson, I. M.; Zuo, J.-M.; Lu, Y. *Nat. Nanotechnol.* **2011**, 6, 93.
- 16 Xie, J.; Zheng, Y.; Ying, J. Y. *J. Am. Chem. Soc.* **2009**, 131, 888.
- 17 Yu, J.; Patel, S. A.; Dickson, R. M. *Angew. Chem., Int. Ed.* **2007**, 46, 2028.
- 18 Wang, Y.; Cui, Y.; Zhao, Y.; Liu, R.; Sun, Z.; Li, W.; Gao, X. *Chem. Commun.* **2012**, 48, 871.
- 19 Zhang, P.; Yang, X. X.; Wang, Y.; Zhao, N. W.; Xiong, Z. H.; Huang, C. *Z. Nanoscale* **2014**, 6, 2261.
- 20 Zheng, J.; Zhang, C.; Dickson, R. M. *Phys. Rev. Lett.* **2004**, 93, 077402.
- 21 Zheng, J.; Petty, J. T.; Dickson, R. M. *J. Am. Chem. Soc.* **2003**, 125, 7780.
- 22 Shang, L.; Dong, S. *Chem. Commun.* **2008**, 1088.
- 23 Wei, H.; Wang, Z.; Yang, L.; Tian, S.; Hou, C.; Lu, Y. *Analyst* **2010**, 135, 1406.
- 24 Rao, T. U. B.; Nataraju, B.; Pradeep, T. *J. Am. Chem. Soc.* **2010**, 132, 16304.
- 25 Wei, W.; Lu, Y.; Chen, W.; Chen, S. *J. Am. Chem. Soc.* **2011**, 133, 2060.
- 26 Yu, Y.; Luo, Z.; Teo, C. S.; Tan, Y. N.; Xie, J. *Chem. Commun.* **2013**, 49, 9740.
- 27 Shang, L.; Dong, S. J.; Nienhaus, G. U. *Nano Today* **2011**, 6, 401.
- 28 Wu, X.; He, X.; Wang, K.; Xie, C.; Zhou, B.; Qing, Z. *Nanoscale* **2010**, 2, 2244.
- 29 Archana, R.; Sonali, S.; Deepthy, M.; Prasanth, R.; Habeeb, M.; Thalappil, P.; Shantikumar, N.; Manzoor, K. *Nanotechnology* **2010**, 21, 055103.
- 30 Chen, T.-H.; Tseng, W.-L. *Small* **2012**, 8, 1912.
- 31 Tao, Y.; Ju, E.; Li, Z.; Ren, J.; Qu, X. *Adv. Func. Mater.* **2014**, 24, 1004.
- 32 Tao, Y.; Lin, Y.; Huang, Z.; Ren, J.; Qu, X. *Adv. Mater.* **2013**, 25, 2594.
- 33 Cui, Y.; Wang, Y.; Liu, R.; Sun, Z.; Wei, Y.; Zhao, Y.; Gao, X. *ACS Nano* **2011**, 5, 8684.
- 34 Tan, Y. N.; Lee, J. Y.; Wang, D. I. C. *J. Am. Chem. Soc.* **2010**, 132, 5677.
- 35 Celej, M. S.; Montich, G. G.; Fidelio, G. D. *Protein Sci.* **2003**, 12, 1496.
- 36 Layton, C. J.; Hellinga, H. W. *Biochemistry* **2010**, 49, 10831.
- 37 It should be mentioned that the reaction temperature was selected as 60 °C because it was the optimal temperature for rapid formation of Au NCs in homogeneous solutions. When the reaction temperature went beyond 60 °C (e.g., 70 °C), HSA would start to form gel due to severe denaturation of the protein which made the drug screening impossible.
- 38 Ghuman, J.; Zunszain, P. A.; Petitpas, I.; Bhattacharya, A. A.; Ottagiri, M.; Curry, S. *J. Mol. Biol.* **2005**, 353, 38.
- 39 Shortridge, M. D. Nuclear magnetic resonance affinity screening methods for functional annotation of proteins and drug discovery. Dissertation/Thesis, The University of Nebraska - Lincoln, Ann Arbor, 2010.